

# Single-Cell Dynamics of Genome-Nuclear Lamina Interactions

Jop Kind,<sup>1,\*</sup> Ludo Pagie,<sup>1</sup> Havva Ortabozkoyun,<sup>1</sup> Shelagh Boyle,<sup>3</sup> Sandra S. de Vries,<sup>1</sup> Hans Janssen,<sup>2</sup> Mario Amendola,<sup>1</sup> Leisha D. Nolen,<sup>3</sup> Wendy A. Bickmore,<sup>3</sup> and Bas van Steensel<sup>1,\*</sup>

<sup>1</sup>Division of Gene Regulation

<sup>2</sup>Electron Microscopy Facility

Netherlands Cancer Institute, Amsterdam, 1066 CX, the Netherlands

<sup>3</sup>MRC Human Genetics Unit, MRC Institute of Genetics and Molecular Medicine, University of Edinburgh, Edinburgh, EH4 2XU, United Kingdom

\*Correspondence: j.kind@nki.nl (J.K.), b.v.steensel@nki.nl (B.v.S.)

<http://dx.doi.org/10.1016/j.cell.2013.02.028>

## SUMMARY

The nuclear lamina (NL) interacts with hundreds of large genomic regions termed lamina associated domains (LADs). The dynamics of these interactions and the relation to epigenetic modifications are poorly understood. We visualized the fate of LADs in single cells using a “molecular contact memory” approach. In each nucleus, only ~30% of LADs are positioned at the periphery; these LADs are in intermittent molecular contact with the NL but remain constrained to the periphery. Upon mitosis, LAD positioning is not detectably inherited but instead is stochastically reshuffled. Contact of individual LADs with the NL is linked to transcriptional repression and H3K9 dimethylation in single cells. Furthermore, we identify the H3K9 methyltransferase G9a as a regulator of NL contacts. Collectively, these results highlight principles of the dynamic spatial architecture of chromosomes in relation to gene regulation.

## INTRODUCTION

It is well established that the positioning of interphase chromosomes within the three-dimensional space of the nucleus is nonrandom, yet it remains unclear how this spatial organization is brought about and what players are involved. One proposed mechanism involves the nuclear lamina (NL), a filamentous protein layer composed of A- and B-type lamins that coats the nucleoplasmic side of the inner nuclear membrane (Prokocimer et al., 2009; Shevelyov and Nurminsky, 2012). The NL provides a large surface area that appears to be an anchoring platform for chromosomes (Chubb et al., 2002; van Steensel and Dekker, 2010). Mapping by means of the DamID technology has revealed that mammalian genomes contain about 1,100–1,400 lamina associated domains (LADs), which are regions of ~0.1–10 Mb that specifically associate with the NL. LADs are relatively gene poor, have a repressive chromatin signature, and are often

demarcated by specific sequence elements (Kind and van Steensel, 2010).

LADs are found on all chromosomes and collectively cover 35%–40% of the mammalian genome (Guelen et al., 2008; Peric-Hupkes et al., 2010). This remarkably large proportion suggests that LAD-NL interactions impose major constraints on the shape and positioning of chromosomes. Hence, much may be learned about chromosome architecture by studying LAD-NL interactions in more detail. For example, knowledge of the dynamics of these interactions throughout the cell cycle may shed light on the plasticity of chromosome folding, and comparison of LAD-NL interactions between mother and daughter cells could address the intriguing question of whether chromosome folding is heritable. In addition, an understanding of the molecular cues that target LADs to the NL will provide insight into some of the mechanisms that determine the overall architecture of chromosomes.

Current knowledge of the dynamics of LAD-NL interactions in individual cells is mostly based on indirect evidence. Fluorescence in situ hybridization (FISH) microscopy of a handful of LADs has indicated that they are indeed preferentially, but not always, located near the NL (Guelen et al., 2008; Peric-Hupkes et al., 2010; Zullo et al., 2012), suggesting that the LAD-NL interactions are dynamic to some degree. However, FISH can only be performed in fixed cells, and due to the limited resolution of light microscopy it is not possible to know whether a LAD makes direct molecular contact with the NL, or is merely nearby. Other approaches, such as tagging of single loci with Lac operon (LacO) arrays, as well as photobleaching and photoactivation experiments, have demonstrated that interphase chromatin is locally mobile but rarely moves over long distances, except during the first 2 hr of G1 phase (Strickfaden et al., 2010; Thomson et al., 2004; Vazquez et al., 2001; Walter et al., 2003). Yet it is not known whether this principle also applies to LADs, which could be firmly anchored to the NL and thereby provide chromosomes with a stable backbone. Furthermore, a few reports have addressed whether the nuclear position of single loci and entire chromosomes is heritable (Gerlich et al., 2003; Strickfaden et al., 2010; Thomson et al., 2004), but it is not clear whether the overall folding state of chromosomes is transmitted from mother to daughter cells.

Likewise, little is known about the mechanisms that drive LAD-NL interactions. Recently it was reported that long  $(GA)_n$  repeats account for the peripheral positioning of certain LADs (Zullo et al., 2012). Besides specific DNA sequences, local chromatin characteristics of LADs may play a role, because a wide range of molecular interactions have been reported between chromatin components and NL proteins (Prokocimer et al., 2009) and methylated histone H3 lysine 9 was found to be important for the NL anchoring of certain genes in *C. elegans* (Towbin et al., 2012).

Here, we report the use of DNA adenine methylation as an artificial epigenetic tag to visualize, track and manipulate LADs in single human cells. A key feature of this approach is that regions of genomic DNA are permanently labeled in living cells once they contact the NL, enabling us to follow their fate over time. Using this method, we demonstrate that LAD-NL contacts are highly dynamic and that positioning of LADs at the NL is determined in an apparently stochastic manner early after mitosis. Furthermore, we find that the stochastic contacts of LADs with the NL are directly linked to gene repression and their level of the histone modification H3K9me2 and that the H3K9 methyltransferase G9a controls the contact frequency of LADs with the NL.

## RESULTS

### $m^6A$ -Tracer Technology

Our method of tracking genome-NL interactions in single cells builds upon the DamID technology, in which genomic regions that are in molecular contact with a nuclear protein of interest are tagged in vivo with adenine-6-methylation ( $m^6A$ ), a modification unknown to higher eukaryotes (van Steensel and Henikoff, 2000). This method was previously used to map genome-NL contacts (Guelen et al., 2008; Pickersgill et al., 2006). Specifically, by expressing a fusion protein consisting of *E. coli* DNA adenine methyltransferase (Dam) and Lamin B1, any DNA in molecular contact with the NL is adenine methylated. Because  $m^6A$  is a stable covalent modification, we reasoned that visualization of this mark inside cells would highlight not only DNA in direct contact with the NL but also any DNA that was adenine methylated in a previous contact event. Hence, this strategy could provide a microscopic “history tracking” of genome-NL interactions.

In order to visualize  $m^6A$  in the genome of intact cells, we required a protein module that specifically recognizes this DNA modification. We reasoned that the restriction endonuclease DpnI, which cuts the sequence  $G^{m^6A}ATC$  but not GATC (Hermann and Jeltsch, 2003), might contain a domain that selectively binds to  $G^{m^6A}ATC$ . Because DpnI has been poorly characterized, we systematically tested eight different truncations of this protein for the desired specificity (Figure 1A). We fused each truncation to enhanced green fluorescent protein (eGFP) and coexpressed it with either Dam-Lamin B1 or Dam-only in the human fibrosarcoma cell line HT1080 (Figure 1B). Four overlapping DpnI truncation fragments yielded a conspicuous nuclear rim staining when coexpressed with Dam-Lamin B1 but not with Dam alone, indicating that they harbor a  $G^{m^6A}ATC$ -binding domain. This is in agreement with the recently reported crystal structure of DpnI (Siwek et al., 2012). We proceeded with truncation #7, a C-terminal fragment of 109 amino acids that illuminated DNA at the

nuclear periphery most consistently when coexpressed with Dam-Lamin B1 (data not shown). We will refer to this fragment fused to eGFP as  $m^6A$ -Tracer.

Biochemical characterization indicated that the affinity of  $m^6A$ -Tracer is much higher for fully adenine-methylated GATC motifs compared to unmethylated or hemimethylated DNA. Even a 1,000-fold excess of unmethylated competitor does not detectably affect binding to fully methylated GATC (Figure 1C). None of the DpnI truncations, including #7, harbor any endonuclease activity (Figure 1D), which would be undesirable for its application in living cells.

To further verify that  $m^6A$ -Tracer, when coexpressed with Dam-Lamin B1, indeed binds LADs, we conducted chromatin immunoprecipitation (ChIP) experiments with an antibody against eGFP. Quantitative PCR (qPCR) of immunoprecipitated material confirmed that  $m^6A$ -Tracer in the presence of Dam-Lamin B1 is enriched in LADs (Figure 1E). Immunofluorescence microscopy showed that Lamin B1 is essentially absent from the nuclear interior in HT1080 cells (Figures S1A and S1B, available online); consistent with this we observe virtually no  $m^6A$ -Tracer signal in the nuclear interior 24 hr after cotransfection of Dam-Lamin B1 and  $m^6A$ -Tracer (Figures S1C and S1D). In contrast, Lamin A is clearly present in the nuclear interior, and Dam-Lamin A yields substantial internal  $m^6A$ -Tracer signals (Figures S1A–S1D). Collectively, these data demonstrate that  $m^6A$ -Tracer, when coexpressed with Dam-Lamin B1, can be used to specifically visualize genomic regions that engage in molecular contact with the NL.

### Interphase LADs Are Mobile within a Narrow Zone underneath the NL

To gain insight into the dynamics of LADs, we generated an HT1080-derived clonal cell line in which both  $m^6A$ -Tracer and Dam-Lamin B1 can be induced independently (Figure 2A). The induction of  $m^6A$ -Tracer is based on the Tet-Off system, where the removal of Doxycycline (Dox) results in the activation of transcription (Gossen and Bujard, 1992). Inducible Dam-Lamin B1 expression was established by the fusion of a destabilization domain (DD) (Banaszynski et al., 2006), which causes Dam-Lamin B1 to be rapidly targeted for proteasomal degradation unless the protein is shielded by the synthetic small molecule Shield1. We refer to this cell line as clone3. Neither the fusion of the DD nor the relatively high expression levels of Dam-Lamin B1—as compared to the standard DamID protocol (Meuleman et al., 2013)—affected the genome-NL interactions (Figure S2A). Furthermore,  $m^6A$ -Tracer and Dam-Lamin B1 expression did not detectably affect cell health, viability, or cell-cycle progression (Figure S2B and Extended Experimental Procedures), nor did it alter local chromatin compaction or the histone modification patterns of LADs (Figures S2C–S2E).

In order to study the dynamics of genome-NL contacts in interphase, we arrested clone3 cells in mitosis by the addition of nocodazole to the medium; after 2 hr, we collected the mitotic cells by mitotic shake-off, released them from the nocodazole block, and induced Dam-Lamin B1 expression. We then monitored the  $m^6A$ -Tracer patterns throughout interphase over 25 hr. Within 5 hr after Dam-Lamin B1 induction, the  $m^6A$ -Tracer signal became visible at the periphery of the nucleus (Figure 2B).

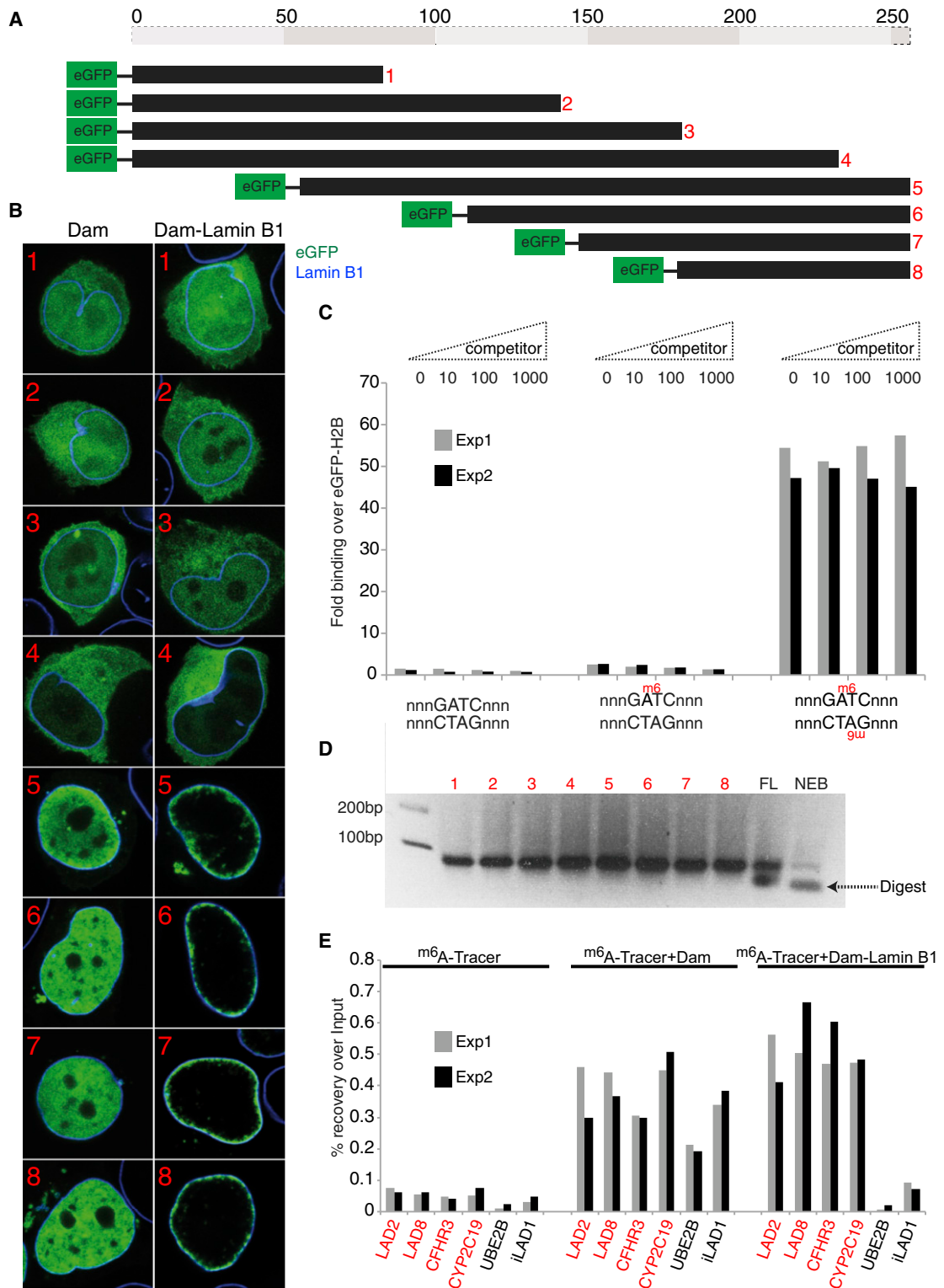


**Figure 1. The <sup>m6</sup>A-Tracer System to Study the Dynamics of NL-Genome Interactions**

(A) Schematic representation of eight DpnI truncations fused to eGFP. Scale bar is in amino acids.

(B) Cellular localization of each eGFP-DpnI truncation upon coexpression with either Dam (left column) or Dam-Lamin B1 (right column).

(C) In vitro <sup>m6</sup>A-binding of eGFP-DpnI truncation #7 to a DNA fragment containing an unmethylated, hemimethylated or fully methylated GATC sequence, in the presence of various amounts (fold excess) of unmethylated competitor DNA. Data from two independent experiments (Exp1 and Exp2) are shown.

(legend continued on next page)

This early signal appeared in patches, but over time most of the NL became lined with a layer of <sup>m6</sup>A-Tracer signal. Interestingly, already at 5 hr, we observed occasional signals that were up to ~1 μm away from the NL, which is evidently too far to be in molecular contact. Such detached signals became progressively more frequent over time (Figure 2B). Because the <sup>m6</sup>A tags are stable, these regions must have contacted the NL at an earlier time point and then moved away from the NL. However, even after 25 hr the vast majority of <sup>m6</sup>A-Tracer signals remained within 1 μm from the NL (Figures 2B and 2C). From these cumulative labeling and tracking experiments we infer that genome-NL contacts during interphase are generally dynamic, because regions that have contacted the NL may move up to ~1 μm from the NL within a few hours. Migration beyond this distance is very rare, suggesting that the mobility of LADs during interphase is confined to a narrow zone near the NL.

It has been suggested that the transcription machinery may play an important role in nuclear organization (Cook, 2010). For example, active genes may be anchored to transcription factories in the nuclear interior, and as a consequence, inactive parts of the genome may be passively driven to the nuclear periphery. We therefore tested whether the peripheral positioning of LADs could be perturbed by inhibition of global transcription. After 24 hr exposure of cells to alpha-amanitin, which causes near-complete shutdown of RNA polymerase II activity, we observed a significant dispersal of <sup>m6</sup>A-Tracer signal (Figures S2F–S2I). However, the overall peripheral distribution was only partially disrupted, suggesting that other mechanisms contribute to the NL confinement of LADs.

### Dynamic Genome-NL Contacts Involve Classical H3K9me2-Marked Heterochromatin

In order to study the nature of the narrow dynamic LAD zone in more detail, we conducted electron microscopy after immunogold labeling of eGFP in U2OS cells cotransfected with Dam-Lamin B1 and the <sup>m6</sup>A-Tracer. Twenty-four hours after transfection, we found <sup>m6</sup>A-Tracer signals predominantly in a layer less than 1 μm from the NL consistent with light microscopy observations (Figures 2D and S2J). The immunogold particles are preferentially found throughout the peripheral electron-dense chromatin material that is classically defined as heterochromatin. Thus, the dynamic contacts of the genome with the NL primarily involve this dense type of heterochromatin. The condensed appearance is not caused by <sup>m6</sup>A-Tracer binding, because coexpression of <sup>m6</sup>A-Tracer with unfused Dam yields immunogold labeling that is mostly located in less electron-dense regions of the nucleus (Figures S2K and S2L).

The histone modification H3K9me2 was previously found at the nuclear periphery of mammalian cell nuclei (Wu et al., 2005; Yokochi et al., 2009) and found to be enriched in LADs (Guelen et al., 2008; Peric-Hupkes et al., 2010; Wen et al., 2009). Staining of clone3 and parental HT1080 cells with an anti-

body against H3K9me2 confirmed that this mark is enriched at the nuclear periphery and generally overlaps with the <sup>m6</sup>A-Tracer signals (Figures 2E and S2M). ChIP of H3K9me2 confirms this enrichment in LADs (Figure S2E). In contrast, the related modification H3K9me3 is less enriched at the periphery, consistent with previous data (Wu et al., 2005; Yokochi et al., 2009), and typically does not overlap with <sup>m6</sup>A-Tracer (Figures 2E and S2M). By ChIP we also did not find H3K9me3 enriched in LADs (Figure S2E). We note, however, that H3K9me3 has been predominantly found at centromeric regions (Peters et al., 2001; Wu et al., 2005), which cannot be detected by the <sup>m6</sup>A-Tracer technology because centromeric repeats lack GATC sequence motifs.

Together, these results indicate that LADs at the nuclear periphery correspond primarily to heterochromatin that appears condensed in transmission electron microscopy and is marked by H3K9me2.

### Disruption of LAD-NL Contacts by Targeting of an Activator

We wondered whether the heterochromatic state of LADs is required for their molecular contacts with the NL. To address this question we made use of the acidic-activating domain (AAD) of the viral protein VP16, which has been reported to disrupt the heterochromatic state and peripheral positioning of an artificial repeat array (Chuang et al., 2006; Tumber et al., 1999). We targeted the AAD specifically to LADs by fusing it to the <sup>m6</sup>A-Tracer and coexpressing it with Dam-Lamin B1. Strikingly, targeting of a tandem array of three copies of this AAD to LADs caused substantial broadening and a more dispersed appearance of the sub-NL zone of <sup>m6</sup>A-Tracer signals (Figures 3A and 3B), even though the integrity of the NL was not visibly affected (Figure 3A). Thus, the VP16 AAD, when targeted to LADs, causes destabilization of the peripheral positioning of LADs. However, not all LADs appear equally sensitive to VP16, because in all nuclei the most peripheral shell retained substantial <sup>m6</sup>A-Tracer signals.

This destabilization of LAD positioning by VP16 is not due to activation of genes within LADs, because messenger RNA sequencing (mRNA-seq) showed very few significant increases in gene expression within LADs after targeting of the AAD for 24 hr (Figure 3C). Because targeted VP16 is known to cause changes in histone modifications (Carpenter et al., 2005), we asked whether increased acetylation of histones might account for the relocation of LADs. By quantitative immunofluorescence microscopy we observed that histone H3 acetylation (H3Ac) increased in LADs when VP16 was fused to <sup>m6</sup>A-Tracer compared to <sup>m6</sup>A-Tracer alone (Figure 3D, first and third column). However, this increase was similar in LADs that remained at the NL, compared to LADs that had moved to the nuclear interior (Figure 3E). It is therefore unlikely that elevated H3ac alone causes detachment of LADs from the NL.

(D) Restriction endonuclease activity of the DpnI truncations and full-length DpnI (fused to eGFP) and commercial pure DpnI (NEB), using a dsDNA fragment containing a single fully methylated GATC sequence as substrate. Arrow points to the digested product.

(E) ChIP of <sup>m6</sup>A-Tracer, without or with coexpression of Dam alone or Dam-Lamin B1, using an antibody against eGFP. Recovery relative to input was determined for four LAD (red) and two inter-LAD (black) sequences (Table S3). Data are from two independent experiments (Exp1 and Exp2). Note that Dam methylates all loci, whereas Dam-Lamin B1 specifically methylates LADs. See also Figure S1 and Table S3.

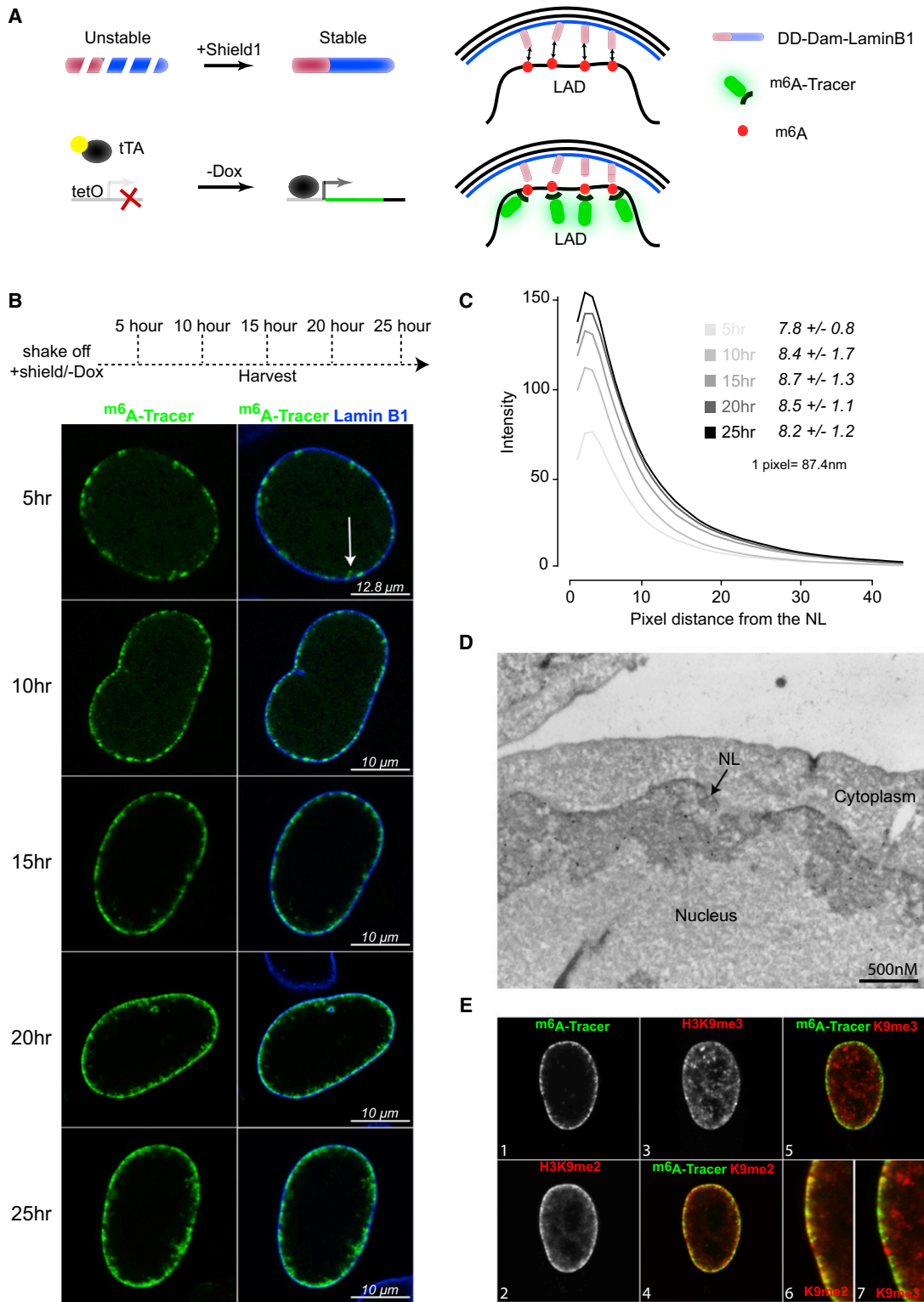


**Figure 2. Confined Dynamics of LADs during Interphase**

(A) Design of the inducible <sup>m6A</sup>-Tracer/Dam-Lamin B1 system.

(B) Representative confocal sections showing accumulation of <sup>m6A</sup>-Tracer signal at the nuclear periphery at indicated times after induction of Dam-Lamin B1 expression, which was started immediately upon the release from a nocodazole block. Note that LADs marked by <sup>m6A</sup>-Tracer (green) can move over short distances from the NL (arrow) but are not typically found in the nuclear interior. Lamin B1 staining is shown in blue.

(legend continued on next page)

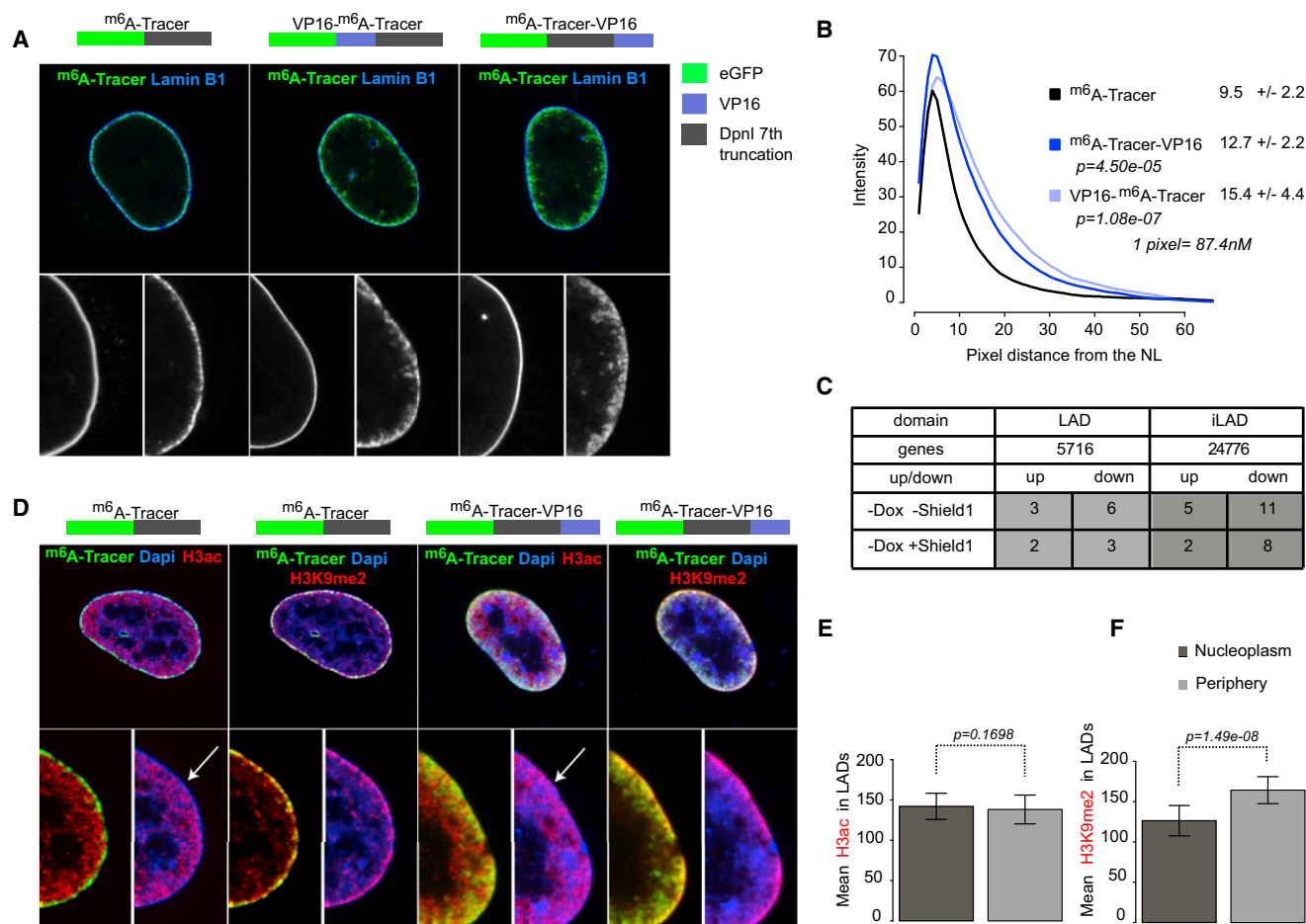


### Figure 3. VP16 Targeting Dislodges LADs from the NL

(A) Representative images showing the displacement of the m<sup>6</sup>A-Tracer signal away from the NL after targeting of the VP16 AAD to LADs (center and right columns) compared to m<sup>6</sup>A-Tracer without the AAD (left column). Note that the displacement is similar for N- and C-terminal AAD fusions. Bottom panels show separate channels at higher magnifications.

(B) Average radial distribution of m<sup>6</sup>A-Tracer signals after induction of the m<sup>6</sup>A-Tracer alone (black line) or fused to the AAD (blue lines). Numbers in the upper-right corner represent average (± SD) distance (in pixels) from the NL at which m<sup>6</sup>A-Tracer signals are at half-maximum intensity (n = 25). *p* value according to an unpaired Wilcoxon test.

(C) Gene expression analysis 24 hr after induction of either m<sup>6</sup>A-Tracer-VP16 alone (top row in gray) or in combination with Dam-Lamin B1 (bottom row in gray) compared to control samples without induction. Numbers in gray boxes indicate genes with significantly altered expression levels.

(D) Immunofluorescence images showing H3ac (red) infiltration into the NL compartment upon AAD targeting (third column, arrow), an environment normally devoid of H3ac (first column, arrow). Second and fourth column, H3K9me2 (red) is reduced on LADs that moved to the nuclear interior after AAD targeting. m<sup>6</sup>A-Tracer is shown in green and DNA in blue.

(E and F) Per-pixel quantification of the H3ac (E) and H3K9me2 (F) intensity levels on LADs located in the nucleoplasm (left bar) and at the NL (right bar). LADs are defined here as m<sup>6</sup>A-Tracer signals with pixel values ≥ 150. Data are represented as mean ± SD (n = 28). *p* value according to a paired Wilcoxon test.

We then investigated the state of H3K9me2. Remarkably, after targeting of VP16, LADs that remained at the nuclear periphery retained H3K9me2, while LADs that relocated to the nuclear interior showed significantly less H3K9me2 (Figure 3D,

second and fourth column; Figure 3F). This correlation is suggestive of a role for H3K9me2 in the retention of LADs near the NL. We therefore propose that alterations in the chromatin state can dislodge LADs from the NL in the absence of gene

(C) Average radial distribution of m<sup>6</sup>A-Tracer signals at indicated times after Dam-Lamin B1 induction (n = 50, except for t = 5 hr with n = 32). Numbers in the upper-right corner represent average (± SD) distance (in pixels) from the NL at which m<sup>6</sup>A-Tracer signals are at half-maximum intensity.

(D) Electron micrograph of a U2OS nucleus after immunogold labeling of m<sup>6</sup>A-Tracer coexpressed with Dam-Lamin B1. Note that gold particles are present throughout heterochromatin, but much less in euchromatin.

(E) Immunofluorescent labeling showing that m<sup>6</sup>A-Tracer (green) after induction of Dam-Lamin B1 colocalizes substantially with H3K9me2 (images 2, 4, and 6) but much less with H3K9me3 (images 3, 5, and 7). See also Figure S2.

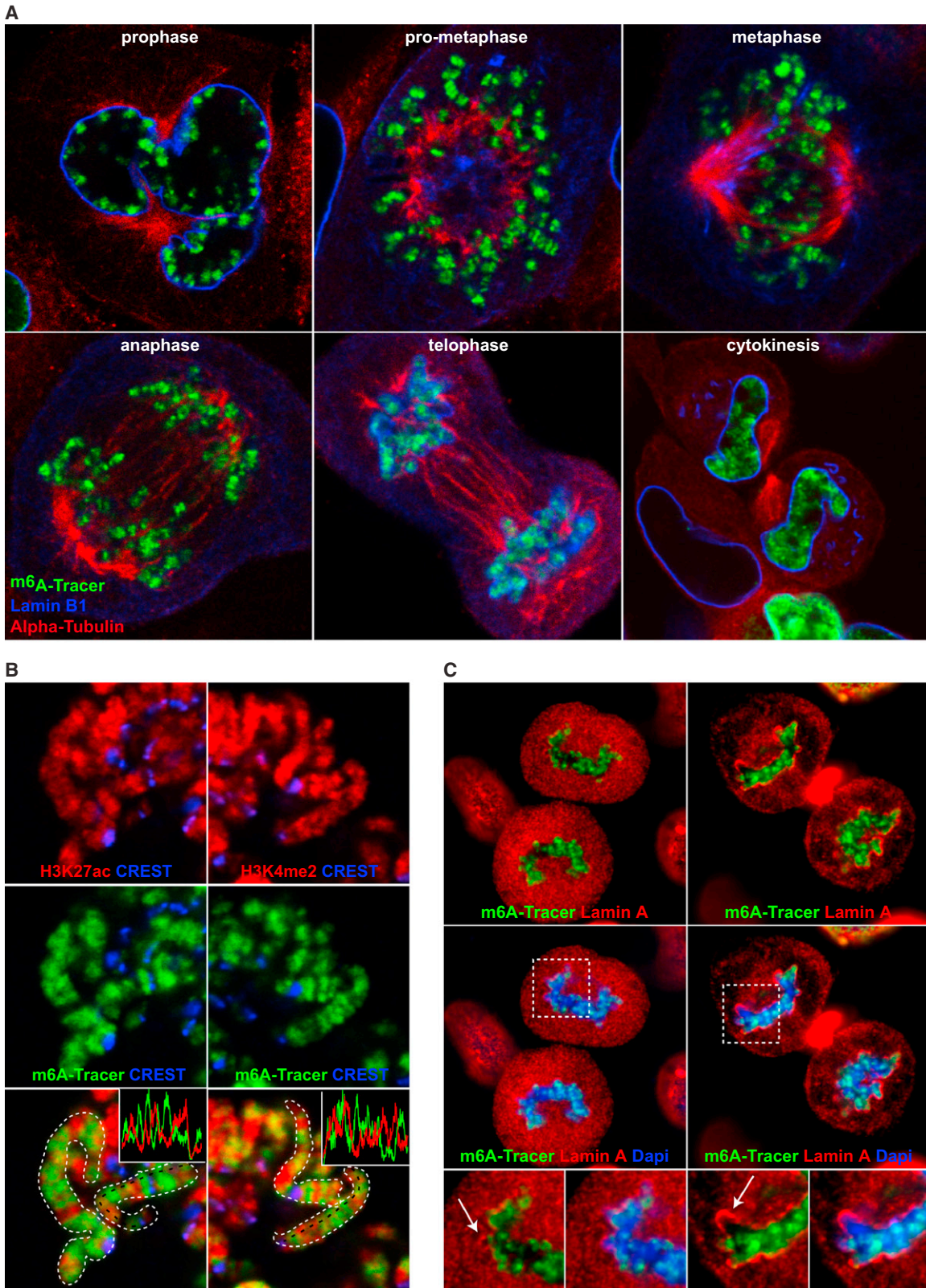


**Figure 4. Fate of LADs during Mitosis**

(A) LAD distribution at different stages of mitosis. Confocal sections show <sup>m6A</sup>A-Tracer (green), Lamin B1 (blue), and alpha-tubulin (red).

(legend continued on next page)

activation. Additional evidence for a causal role of H3K9me2 will be presented below.

### LADs Form Discrete Metaphase Chromosome Bands but Do Not Nucleate NL Reassembly in Telophase

To investigate the fate of LADs during mitosis, we activated Dam-Lamin B1 in unsynchronized clone3 cells with Shield1 for 20 hr, after which we fixed the cells and counterstained with antibodies against alpha-tubulin and Lamin B1, which enabled us to identify cells in specific stages of mitosis (Figure 4A). In prophase, LADs become condensed and rounded, presumably reflecting the ongoing chromosomal compaction. Strikingly, in prometaphase and metaphase (when the NL is disassembled), LADs form a clear banded pattern along the condensed chromosomes (Figure 4A). This pattern alternates with active histone marks such as H3K27ac and H3K4me2 (Figure 4B), indicating that the spatial segregation of LADs and transcriptionally active regions during interphase is largely preserved in mitotic chromosomes. The LAD bands typically span the entire width of metaphase chromosomes, with no apparent preferential radial positioning.

At the anaphase-telophase transition, the NL is reassembled at the surface of the chromosomes (Moir et al., 2000). Recently, an ectopically integrated LAD-derived element was reported to act as a nucleation site for NL assembly (Zullo et al., 2012). In order to test whether endogenous LADs generally perform this function, we analyzed the location of Lamin A relative to the <sup>m6</sup>A-Tracer signals in early and late telophase cells. Confocal microscopy imaging showed deposition of Lamin A along most of chromosomal surface in late telophase but without any detectable preference for LADs (Figure 4C, see arrows in bottom panels). Thus, in general, chromosomal regions that were LADs in the mother cell do not act as preferred nucleation points for initial NL assembly in the daughter cells.

### Stochastic Reshuffling of LADs after Mitosis

Even though the newly formed NL shows no preference for LADs in telophase, we hypothesized that LADs would return to the NL early in G1 phase, when chromatin is highly mobile (Dimitrova and Gilbert, 1999; Thomson et al., 2004). To monitor this, we conducted time-lapse microscopy of the <sup>m6</sup>A-Tracer, using Red Fluorescent Protein-tagged histone H2B (H2B-mRFP) to simultaneously visualize bulk chromatin. Dam-Lamin B1 expression was induced for 20 hr prior to imaging of telophase cells. We thus could specifically track the LADs that had been in contact with the NL in the mother cells (“mother LADs”) and study their fate in early G1 of the daughter cells. The results revealed that in telophase most mother LADs are not yet positioned at the periphery of the newly formed nuclei (Figures 5A and S3A). Only after ~40 min into G1 phase, a subset of LADs appears to reassociate with the NL (Figure 5A). However, many of the mother LADs do not return to the NL; even 5 hr after mitosis, we found the majority of <sup>m6</sup>A-Tracer signal to be more than 1 μm from the nuclear rim (Figure 5B). These internal signals

show a modest preference to be located close to nucleoli (Figures 5B and 5C).

To ensure that the <sup>m6</sup>A-Tracer itself does not hamper the reassociation of mother LADs with the NL after mitosis, we also activated Dam-Lamin B1 prior to mitosis and turned on <sup>m6</sup>A-Tracer expression only early in G1 of the next cell cycle, i.e., after LAD positioning had stabilized. Again, in the daughter cells many mother LADs were located in the nuclear interior (Figure S3B), indicating that the failure of individual LADs to localize to the NL is not caused by <sup>m6</sup>A-Tracer binding. We therefore conclude that the peripheral positioning of LADs after mitosis is a rather erratic process.

The apparent stochastic association of LADs with the NL raised the question of what proportion of all LADs are NL associated on average. In order to quantify this, we performed DNA FISH with a pool of ~140 × 10<sup>5</sup> oligonucleotides designed to simultaneously detect 25 LADs distributed over most chromosomes (Table S1). This revealed that on average 32.0% ± 11.6% (mean ± SD) of these LADs is located in close proximity (less than 1 μm) to the NL (Figures 5D and 5E).

If the LAD-NL contacts after mitosis are established in a purely stochastic manner, then after every cell division each LAD should have a renewed chance to associate with the NL. Because the <sup>m6</sup>A tags deposited by Dam-Lamin B1 are stable, this predicts that the pool of LADs should acquire additional <sup>m6</sup>A with each new mitosis (provided that Dam-Lamin B1 is continuously expressed). We tested this by quantitative measurements of <sup>m6</sup>A in several LADs over time in synchronized cell populations that express Shield1-inducible Dam-Lamin B1. The <sup>m6</sup>A levels were determined using the restriction endonuclease DpnII (van Steensel and Henikoff, 2000), which specifically cuts unmethylated but not hemimethylated or fully methylated GATC sequences (Hermann and Jeltsch, 2003) (see Table S2 for an overview of the <sup>m6</sup>A assays used). We initially monitored accumulation of <sup>m6</sup>A during the first interphase when Dam-Lamin B1 expression was switched on. In agreement with the <sup>m6</sup>A-Tracer microscopy time series (Figure 2B), the <sup>m6</sup>A levels of individual LADs (but not of inter-LAD regions) increased over time; however, after 15 hr a plateau was reached (Figures 5F and S3C), indicating that all LAD sequences in the peripheral dynamic zone had touched the NL and were fully methylated. When cells were subsequently allowed to go through another mitosis, the cumulative <sup>m6</sup>A levels of each tested LAD nearly doubled in the next interphase (Figure 5G). This doubling indicates that NL association in the daughter cells involves a LAD subset that is largely different from the LAD subset that had contacted the NL in the mother cells.

Lastly, we asked whether the stochastic “decision” to position a LAD at the periphery is made independently for each of the two daughter cells or instead is somehow coordinated. By systematic scoring of LAD FISH signals in pairs of daughter cells, we found no significant correlation between the radial positions in the two daughter cells (Figures S3D and S3E). This corroborates

(B) Distribution of LADs (green) in relation to H3K27ac (red, left panel) or H3K4me2 (red, right panel). CREST antibody (blue) marks centromeric regions. Insets show line scans along the chromosomal axis.

(C) Lamin A (red) during early (left panel) and late (right panel) telophase reassembles onto chromosomes (blue) but shows no preference for LADs (green). Arrows mark some Lamin A-rich regions devoid of LADs.

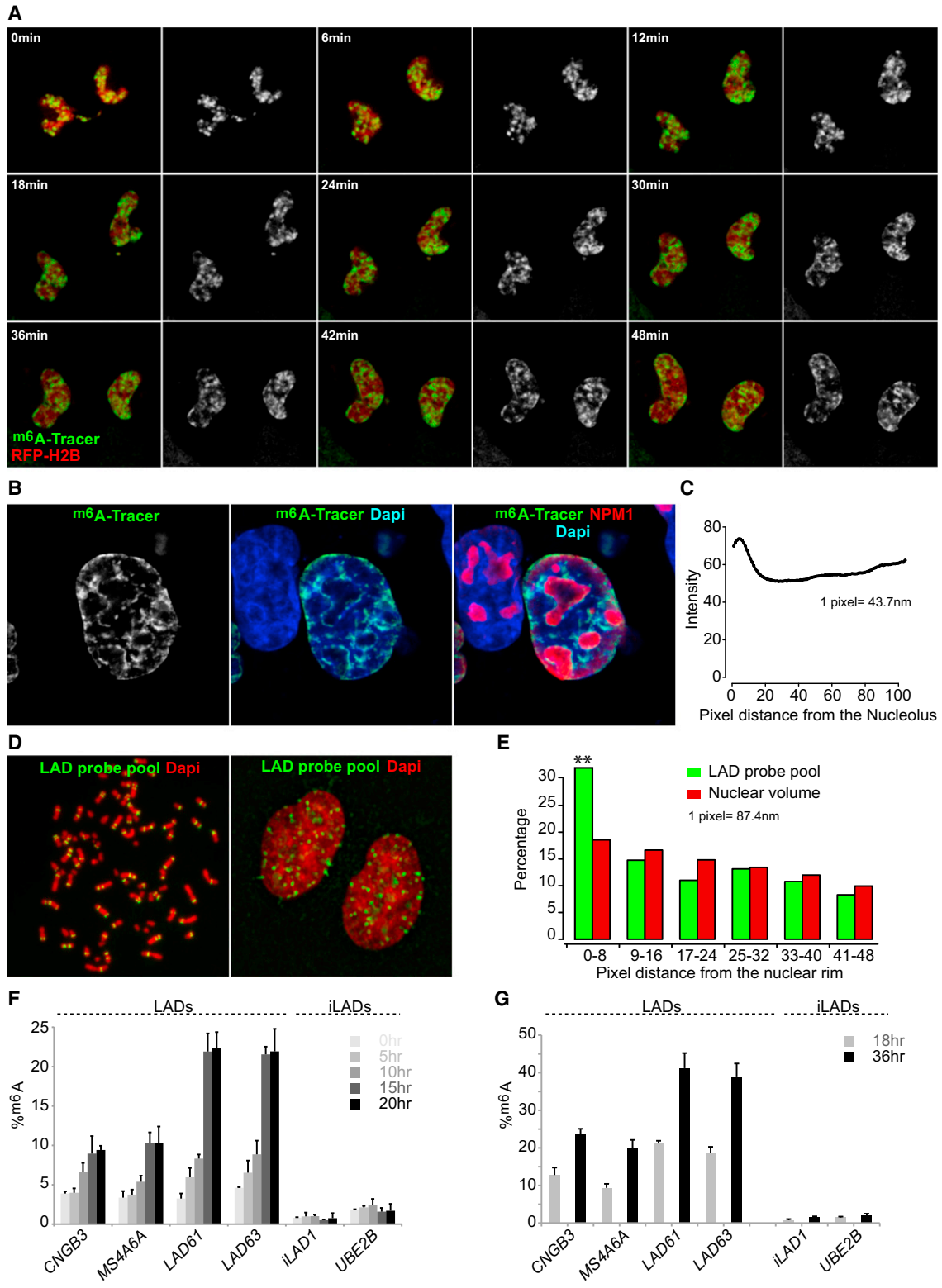


**Figure 5. Reorganization of LADs after Mitosis**

(A) Time-lapse imaging of LADs (green and grayscale) and Histone H2B (red) starting from late telophase.

(B) Organization of LADs (<sup>m6A</sup> deposited by Dam-Lamin B1 expression in the mother cell) in a representative daughter cell about 5 hr after mitosis. Nucleoli are labeled using an antibody against nucleophosmin (NPM1; red).

(legend continued on next page)

earlier observations for laco-tagged loci (Thomson et al., 2004) and underscores that the peripheral position of LADs after mitosis is largely determined by a stochastic mechanism.

### H3K9me2 State of LADs Is Directly Linked to Stochastic Positioning

Given the enrichment of H3K9me2 at the nuclear periphery (Figure 2E) (Wu et al., 2005; Yokochi et al., 2009) and the conspicuous loss of this mark on the dislodged LADs after AAD targeting (Figures 3D and 3F), we asked whether the naturally occurring stochastic contacts with the NL are related to the H3K9me2 status of the LADs. We developed an approach that enabled us to infer a direct relationship—at the level of LAD copies in individual cells—from population-based measurements. As before, we isolated mitotic cells, activated Dam-Lamin B1 expression by treatment with Shield1, and harvested the cells 18 hr later, i.e., before the next mitosis. We collected chromatin from these cells and performed ChIP with antibodies directed against H3K9me2 (or total H3 as a control). On this immunopurified material we then conducted the DpnII-based assay to estimate NL contact frequencies, enabling us to test whether the stochastic NL contacts are linked to variation in H3K9me2 levels (Table S2). Remarkably, seven out of eight LADs show a significantly higher propensity to be associated with the NL when enriched for H3K9me2, than when not (Figure 6A). A striking example is the promoter region of *CDH12*, which is found at the NL in 58% of the cases when modified by H3K9me2, as compared to a general frequency of 25% (Figure 6A, first panel). The same experiment conducted in parallel without Shield1 shows that the protection of DNA against digestion by DpnII is due to the presence of <sup>m6</sup>A and not due to the inability of the enzyme to digest formerly formaldehyde cross-linked material (Figure S4A). These findings imply that the stochastic positioning of a LAD is directly linked to cell-to-cell or allele-to-allele variation in the H3K9me2 level of this LAD (see Discussion).

### The H3K9 Methyltransferase G9a Promotes Lad-NL Contacts

We next tested whether H3K9me2 is required for LAD-NL associations. In mammals, a heteromeric complex of the histone lysine methyltransferases (HKMTs) G9a and GLP1 is primarily responsible for H3K9 dimethylation (Shinkai and Tachibana, 2011). We used RNA interference (RNAi) to knock down G9a and confirmed that this lowered the overall H3K9me2 levels (Figures S4B and S4D), as was reported previously (Tachibana et al., 2005; Yokochi et al., 2009). Strikingly, this caused all eight tested LADs to be less frequently associated with the NL

compared to control-treated cells (Figure 6B). A similar effect was observed after treatment with BIX01294, an inhibitor of the HKMT activity of both G9a and GLP1 (Kubicek et al., 2007; Quinn et al., 2010) (Figure 6B). We found no additional effect when the G9a knockdown was combined with BIX01294 treatment (Figure 6B). In contrast, overexpression of mCherry-tagged G9a caused increased overall H3K9me2 levels and enhanced NL interactions (Figures 6B, S4C, and S4E). The magnitude of this effect may be limited by the availability of the G9a dimerization partner GLP1. In summary, we conclude that G9a modulates LAD-NL contacts, presumably through dimethylation of H3K9.

### “Leaky” LAD Genes Are More Active when Located Away from the NL

While most genes in LADs are expressed at undetectable or very low levels, a small proportion produce substantial amounts of mRNA (Figure 7A). We asked whether these “leaky” LAD genes might become derepressed in particular when stochastically located in the nuclear interior. To address this question we first visualized mother LADs in daughter cells together with H3K4me3. We found that this marker of transcriptional activity is generally low in mother LADs, both at the periphery and nuclear interior (Figure 7B). However, some overlap of internal LADs and H3K4me3 could be detected, and quantitative image analysis suggested slightly higher overall levels of H3K4me3 on internal mother LADs compared to peripheral mother LADs (Figure 7C). Although we note that this overlap may be overestimated due to the resolution of confocal microscopy, this result suggests that some genes within LADs may become active when located in the nuclear interior.

To investigate this at molecular resolution, we repeated the ChIP-DamID experiments as in Figure 6, but this time using an antibody against H3K36me3, which is a marker of transcriptional elongation (Bannister et al., 2005). We focused on five LAD genes with detectable expression according to mRNA-seq (Figure 7A). Strikingly, <sup>m6</sup>A levels deposited on these genes by Dam-Lamin B1, again measured in mother cells prior to mitosis, were consistently lower in the H3K36me3-positive chromatin fraction compared to the total H3-containing fraction (Figure 7D). Note that this result is exactly opposite to that obtained for H3K9me2 (Figure 6A). We conclude that the H3K36me3 state (and thus presumably the transcription activity) of these genes is higher in cells in which the respective LADs are not in contact with the NL. This implies that contact of these genes with the NL is inversely linked to stochastic variation of their expression in the population of cells.

(C) Average distribution of <sup>m6</sup>A-Tracer signals in daughter cells (n = 39) as a function of distance to the nearest nucleolus. Positions less than 1.4 μm from the NL were excluded from this analysis.

(D) FISH of 25 LADs (Table S1) in metaphase (left panel) and interphase (right panel).

(E) Radial distribution of FISH signals (n = 29 nuclei). \*\*p < 0.001 according to a paired Wilcoxon test.

(F) Quantitative analysis of <sup>m6</sup>A accumulation within one interphase at indicated time points after Dam-Lamin B1 induction, which was initiated simultaneously with the release from a nocodazole block. Data were generated in clone11 cells that do not express <sup>m6</sup>A-Tracer; a similar result was obtained in clone3 cells that do express <sup>m6</sup>A-Tracer (Figure S3C).

(G) Same as in (F) except that Dam-Lamin B1 was induced for either 18 hr (gray bars), when <sup>m6</sup>A deposition is due to NL interactions in mother cells, or 36 hr (black bars), when <sup>m6</sup>A levels are the cumulative result of NL interactions in mother and daughter cells. Data are represented as mean ± SD (n = 3). See also Figure S3 and Tables S1, S2, and S3.

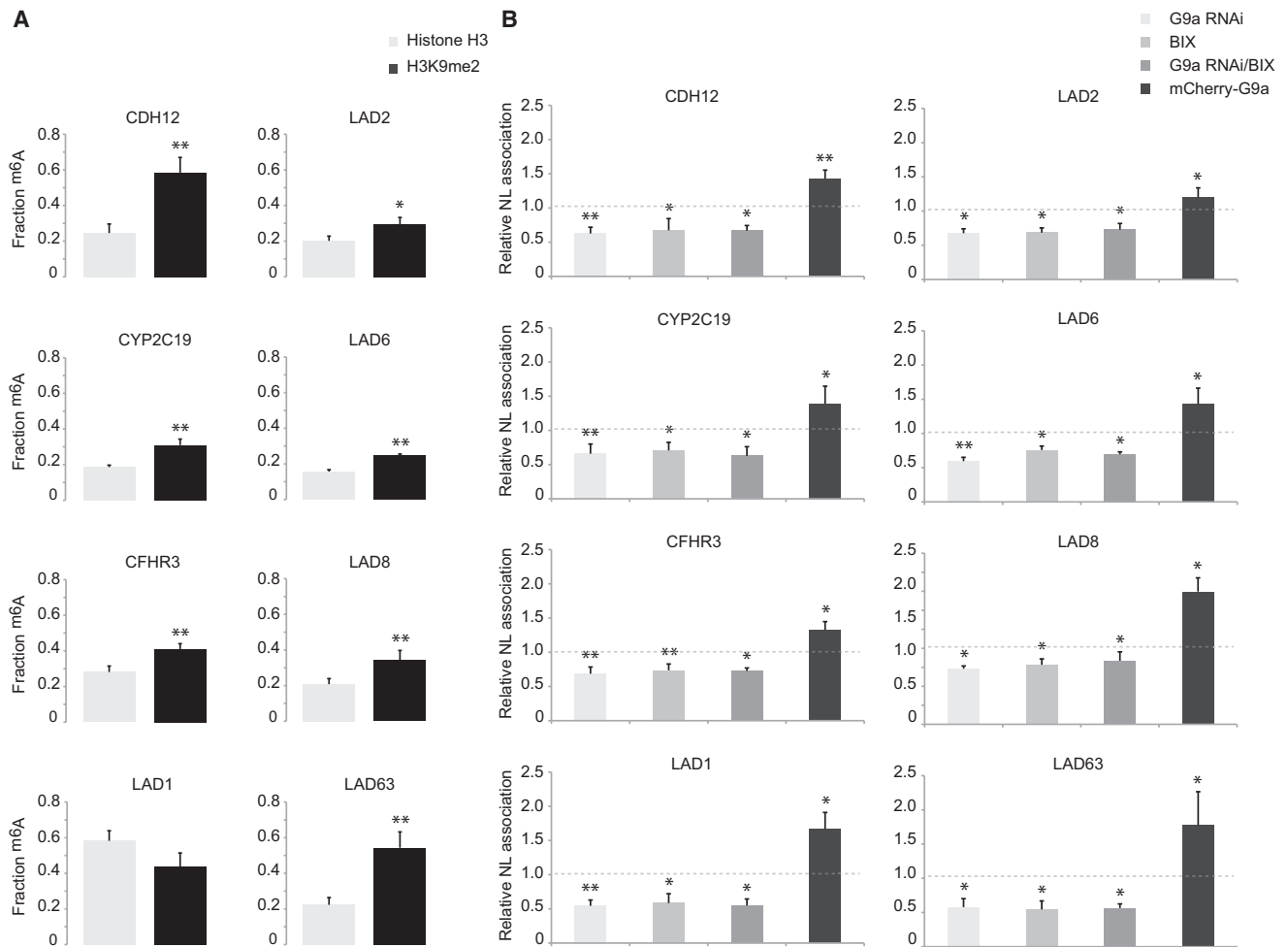


**Figure 6. H3K9me2 by G9a Mediates LAD-NL Associations**

(A) Stochastic NL interactions are linked to H3K9me2 status. Chromatin from Dam-Lamin B1-expressing cells was subjected to ChIP with antibodies directed against Histone H3 (gray) or H3K9me2 (black), followed by quantification of  $m^6A$  levels (representing NL contact frequencies), in eight LADs ( $n = 3$ ). (B) G9a controls LAD-NL interactions. Bars show fold change in NL contact frequencies of eight LADs upon siRNA-mediated knockdown of G9a (G9a RNAi), G9a inhibition by BIX01294 (BIX), a combination of G9a siRNA and BIX01294 (G9a RNAi/BIX), or overexpression of Cherry-G9a (Cherry-G9a). Data are based on four biological replicates and represented as mean  $\pm$  SD. \* $p < 0.05$ , \*\* $p < 0.01$  according to a paired t test. See also Figure S4 and Tables S2 and S3.

## DISCUSSION

Here we demonstrated the use of a “molecular contact memory” approach to follow the fate of NL-genome contacts over time and to identify a role for H3K9me2 in the stochastic positioning of LADs at the periphery.

### Tracking and Targeting of Native Genomic Loci by $m^6A$ -Tracer

We have harnessed DNA adenine methylation as an artificial epigenetic mark to track and manipulate genome-NL contacts in single human cells. Because  $m^6A$  is a stable modification, we could use the combination of inducible Dam-Lamin B1 and  $m^6A$ -Tracer constructs as a “history tracking” system to follow the fate of genomic regions that contact Lamin B1 at a certain point in time. In addition, we demonstrated that these regions

can be collectively manipulated by the fusion of a transcription activator to the  $m^6A$ -Tracer. We expect that various other chromatin regulators and cofactors may be directed in a similar fashion. Moreover, because  $m^6A$  can be specifically deposited at target loci of a wide range of chromatin proteins (Filion et al., 2010), the  $m^6A$ -Tracer system may be applicable to study many aspects of chromatin biology.

### Constrained Mobility of LADs during Interphase

Our results show that within interphase, contacts of the genome with the NL are dynamic. Nevertheless, during interphase loci generally do not migrate far from the NL after a contact event. This constrained mobility of chromatin is in agreement with previous studies that employed photobleaching of nuclear regions or fluorescent tagging of single loci (Abney et al., 1997; Chubb et al., 2002; Vazquez et al., 2001), although these studies

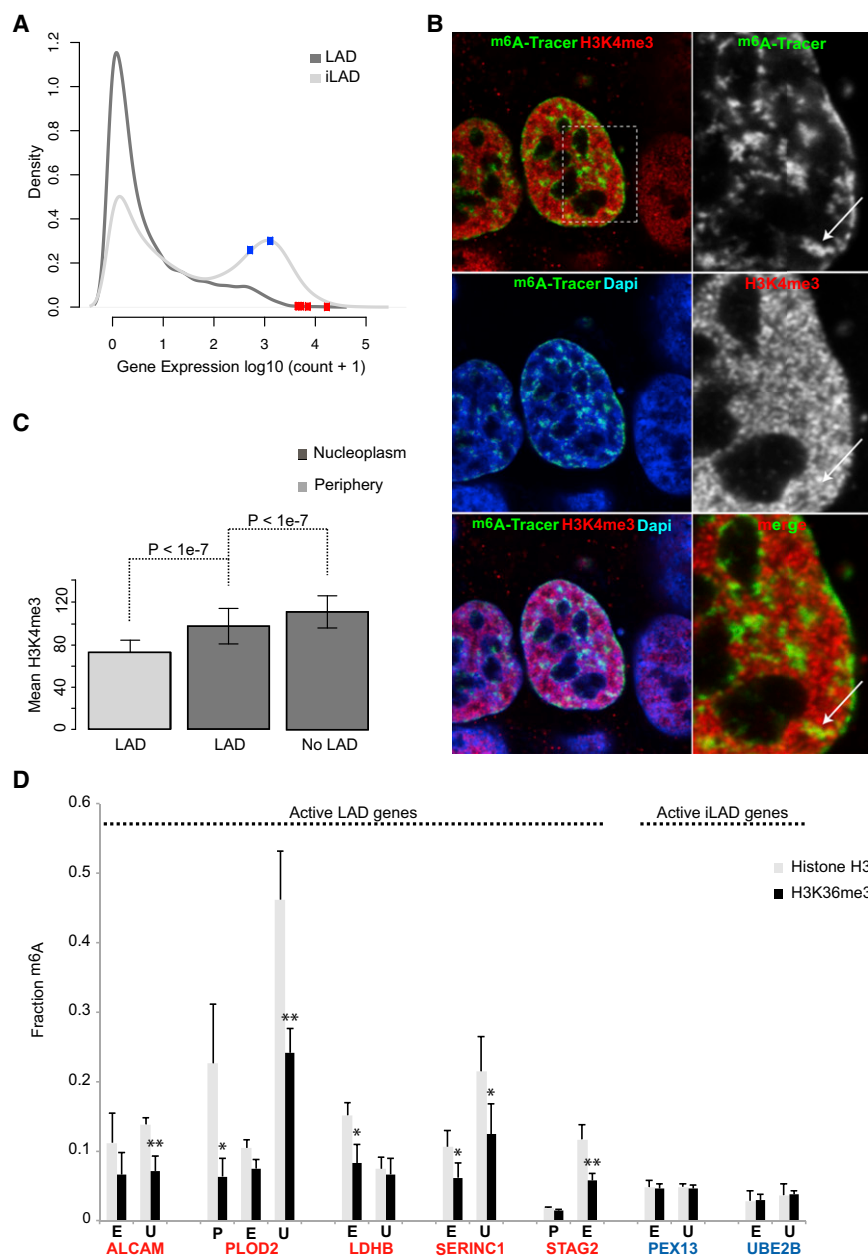


**Figure 7. Dissociation of LADs from the NL Can Be Associated with Gene Activation**

(A) Distribution of gene expression levels in LADs and inter-LADs (iLADs) based on mRNA-seq of uninduced (+Dox/-Shield1) cells as described in Figure 3C. Squares indicate the expression levels of five active LAD (red) and two active iLAD (blue) genes.

(B) Partial overlap of H3K4me3 with internal LADs. Dam-Lamin B1 was expressed in mother cells; daughter cells were fixed 5 hr after mitosis and stained for H3K4me3 (red). Right-hand panels show higher magnification of the left panels. Arrow marks a LAD region that overlaps with H3K4me3 signal.

(C) Quantitative analysis of mean H3K4me3 pixel value distributions in daughter cells as in (B) ( $n = 25$ ) for regions covered by  $m^6A$ -Tracer signals (LADs) or not (No LAD). Light gray: less than or equal to  $1.4 \mu\text{m}$  from the NL; dark gray: more than  $1.4 \mu\text{m}$  from the NL.  $p$  value is according to a paired Wilcoxon test.

(D) Stochastic NL interactions of active LAD genes are inversely linked to their H3K36me3 status. Chromatin from Dam-Lamin B1-expressing mother cells was subjected to ChIP with antibodies directed against Histone H3 (gray) or H3K36me3 (black), followed by quantification of  $m^6A$  levels (representing NL contact frequencies) in promoter (P), exon (E), and 3' UTR (U) regions of five active genes located in LADs (red) and two active genes in iLADs (blue) (Table S3). Note the generally lower NL contact frequencies of LAD gene copies that carry H3K36me3 as compared to bulk (H3 control ChIP) ( $n = 3$ ). Data are represented as mean  $\pm$  SD. \* $p < 0.05$ , \*\* $p < 0.01$  according to a paired  $t$  test. See also Tables S2 and S3.

were not able to detect direct molecular contacts with the NL. Our electron microscopy data indicate that the mobility of peripheral LADs is largely confined to the layer of densely staining heterochromatin. Thus, although the mobility of chromatin within this layer is high, it rarely mixes with the neighboring euchromatin.

#### Activator-Induced Repositioning of LADs

We demonstrated that targeting of the VP16 AAD can drive the “escape” of a subset of LADs from the nuclear periphery, most likely through alterations in the chromatin state rather than through activation of gene expression. This is consistent with the AAD-driven relocation of a single Laco-tagged locus in chinese hamster

cells (Tumbar and Belmont, 2001) and the reported erasure of H3K9me3 at a Laco-tagged locus by VP16 targeting (Hathaway et al., 2012). Hundreds of LAD regions were previously found to relocate relative to the NL upon cellular differentiation; in many instances this occurred in the absence of changes in gene expression (Peric-Hupkes et al., 2010). It is possible

#### Reshuffling of LADs after Mitosis

After mitosis, LADs are stochastically reshuffled, indicating that positioning of genomic loci relative to the NL is generally not heritable. Mother-to-daughter cell transmission of radial positioning is also not supported by a study of two Laco-tagged loci (Thomson et al., 2004) or by anecdotal observations based on the labeling of peripheral chromatin by photoactivation (Strickfaden et al., 2010).

We observed that some of the mother LADs that end up in the nuclear interior after mitosis become closely associated with

nucleoli. Genome-wide mapping studies have found that nucleolus-associated domains (NADs) overlap substantially with LADs (Németh et al., 2010; van Koningsbruggen et al., 2010). It is possible that each LAD/NAD has a distinct distribution probability between nucleoli and the NL.

### NL Interactions of LADs Are Linked to Stochastic Histone Modifications

Our results indicate that the stochastic NL contacts of individual LAD copies are closely linked to their H3K9me2 state. Furthermore, for five active genes embedded in LADs we found that the H3K36me3 state (and thus presumably the transcription state [Bannister et al., 2005]) is inversely linked to stochastic NL contacts. These results imply that the histone modification state of individual LADs is also stochastic, i.e., it must exhibit considerable cell-to-cell variation or allele-to-allele variation in single cells or both. No technique is presently available to directly detect histone modifications on individual loci in single cells. However, di- and trimethylated H3K9 have previously been linked to the variegated expression of reporter genes embedded in heterochromatin, which could point to stochastic variation of these histone marks themselves (Fodor et al., 2010).

Stochastic expression of genes is well documented but the underlying mechanisms are still poorly understood (Lionnet and Singer, 2012; Raj and van Oudenaarden, 2009). Contact of a LAD with the NL may help to repress the genes within this LAD, which is consistent with studies showing that artificial anchoring of genes to the NL can lead to reduced transcriptional activity (Dialynas et al., 2010; Finlan et al., 2008; Reddy et al., 2008). The mechanism of NL-mediated repression still remains to be elucidated.

### G9a Promotes NL Contacts

Our study indicates a role of G9a in promoting LAD-NL contacts, presumably via H3K9me2. Importantly, a recent study in *C. elegans* also found evidence for a role of H3K9 methylation in the targeting of genomic regions to the NL (Towbin et al., 2012). In contrast, a FISH study in mouse embryonic stem cells found no significant change in the peripheral localization of a number of late-replicating G9a target genes after knockout of G9a (Yokochi et al., 2009). This difference may be explained by species- or cell-type specific effects, or by technological differences, because our approach detects molecular contacts whereas DNA-FISH is limited by the resolution of light microscopy.

We cannot rule out the possibility that positioning of LADs at the NL also enforces H3K9me2, i.e., that the causal relationship is circular. If this is the case, it would establish a positive feedback loop that would enforce the H3K9me2-positive state and keep peripherally located LADs at the NL during interphase (Towbin et al., 2012). Although G9a was recently found to interact with the NL-interacting protein BAF (Montes de Oca et al., 2011), we are not aware of direct evidence that G9a or other H3K9 methyltransferases are preferentially active at the NL.

Together, the results reported here provide a foundation for further studies of the relationships between dynamic chromosome organization and transcription regulation in single cells.

## EXPERIMENTAL PROCEDURES

Detailed methods are described in the [Extended Experimental Procedures](#).

### Cell Lines

Stable clonal cell lines were derived from HTC75, which is an HT1080 line that stably expresses the Tet-off transactivator (van Steensel and de Lange, 1997). The Shield1-inducible Dam-Lamin B1 clonal line clone11 was derived by transfecting HTC75 cells with pTuner-DD-Dam-Lamin B1; the <sup>m6</sup>A-Tracer line clone3 was derived from clone11 by transfection with an <sup>m6</sup>A-Tracer expression vector under a Tet-off responsive promoter. Stable clonal cell lines expressing the <sup>m6</sup>A-Tracer-VP16 fusion constructs were created as described for the clone3 line.

### <sup>m6</sup>A-Tracer Microscopy and FISH

Images of fixed cells were taken on Leica TCS SP2 or SP5 microscopes. For time-lapse imaging, clone3 cells were transfected with H2B-mRFP and imaged on a Leica TCS SP5 confocal laser-scanning microscope with a 37°C climate chamber. 3D DNA-FISH was performed as described (Boyle et al., 2011), using a custom-made Texas Red-labeled probe pool consisting of ~140,000 oligonucleotides of an average TM of 76°C that tile each of the 25 LADs. Genomic positions of the probed LADs are listed in [Table S1](#). To visualize a single LADs in both daughter cells we generated a probe with a fosmid (W12-1931L04) that corresponds to the region chr3:136427835-136466953 (GRCh37/hg19).

### ChIP-<sup>m6</sup>A Assay

Clone11 cells were arrested for 4 hr and collected by mitotic shake-off. Then Dam-Lamin B1 expression was induced by addition of Shield1 for 18 hr. Cells were fixed with formaldehyde, chromatin was prepared and subjected to ChIP using antibodies as indicated, precipitated DNA was purified and treated with or without DpnII, after which qPCR across individual GATC sites was done with primers listed in [Table S3](#).

## ACCESSION NUMBERS

Genome-wide DamID and RNA-seq data are available from the Gene Expression Omnibus (<http://www.ncbi.nlm.nih.gov/geo/>), accession number GSE40112.

## SUPPLEMENTAL INFORMATION

Supplemental Information includes four figures, three tables, and Extended Experimental Procedures and can be found with this article online at <http://dx.doi.org/10.1016/j.cell.2013.02.028>.

## ACKNOWLEDGMENTS

We thank Wouter Meuleman for help with FISH probe pool design; Federica Morettini for the scoring of FISH images; the NKI Genomics Core Facility for microarray hybridizations and RNA-seq; and the Wolthuis and Neefjes laboratories for reagents. This work was supported by EMBO LTF and NWO-ALW VENI (J.K.), NWO-ALW VICI and ERC Advanced grant 293662 (B.v.S.), and MRC and ERC Advanced grant 249956 (W.A.B.).

Received: August 30, 2012

Revised: December 17, 2012

Accepted: February 5, 2013

Published: March 21, 2013

## REFERENCES

Abney, J.R., Cutler, B., Fillbach, M.L., Axelrod, D., and Scalettar, B.A. (1997). Chromatin dynamics in interphase nuclei and its implications for nuclear structure. *J. Cell Biol.* 137, 1459–1468.

- Banaszynski, L.A., Chen, L.C., Maynard-Smith, L.A., Ooi, A.G., and Wandless, T.J. (2006). A rapid, reversible, and tunable method to regulate protein function in living cells using synthetic small molecules. *Cell* 126, 995–1004.
- Bannister, A.J., Schneider, R., Myers, F.A., Thorne, A.W., Crane-Robinson, C., and Kouzarides, T. (2005). Spatial distribution of di- and tri-methyl lysine 36 of histone H3 at active genes. *J. Biol. Chem.* 280, 17732–17736.
- Boyle, S., Rodesch, M.J., Halvensleben, H.A., Jeddloh, J.A., and Bickmore, W.A. (2011). Fluorescence in situ hybridization with high-complexity repeat-free oligonucleotide probes generated by massively parallel synthesis. *Chromosome Res.* 19, 901–909.
- Carpenter, A.E., Memedula, S., Plutz, M.J., and Belmont, A.S. (2005). Common effects of acidic activators on large-scale chromatin structure and transcription. *Mol. Cell Biol.* 25, 958–968.
- Chuang, C.H., Carpenter, A.E., Fuchsova, B., Johnson, T., de Lanerolle, P., and Belmont, A.S. (2006). Long-range directional movement of an interphase chromosome site. *Curr. Biol.* 16, 825–831.
- Chubb, J.R., Boyle, S., Perry, P., and Bickmore, W.A. (2002). Chromatin motion is constrained by association with nuclear compartments in human cells. *Curr. Biol.* 12, 439–445.
- Cook, P.R. (2010). A model for all genomes: the role of transcription factories. *J. Mol. Biol.* 395, 1–10.
- Dialynas, G., Speese, S., Budnik, V., Geyer, P.K., and Wallrath, L.L. (2010). The role of *Drosophila* Lamin C in muscle function and gene expression. *Development* 137, 3067–3077.
- Dimitrova, D.S., and Gilbert, D.M. (1999). The spatial position and replication timing of chromosomal domains are both established in early G1 phase. *Mol. Cell* 4, 983–993.
- Filion, G.J., van Bommel, J.G., Braunschweig, U., Talhout, W., Kind, J., Ward, L.D., Brugman, W., de Castro, I.J., Kerkhoven, R.M., Bussemaker, H.J., and van Steensel, B. (2010). Systematic protein location mapping reveals five principal chromatin types in *Drosophila* cells. *Cell* 143, 212–224.
- Finlan, L.E., Sproul, D., Thomson, I., Boyle, S., Kerr, E., Perry, P., Ylstra, B., Chubb, J.R., and Bickmore, W.A. (2008). Recruitment to the nuclear periphery can alter expression of genes in human cells. *PLoS Genet.* 4, e1000039.
- Fodor, B.D., Shukeir, N., Reuter, G., and Jenuwein, T. (2010). Mammalian Su(var) genes in chromatin control. *Annu. Rev. Cell Dev. Biol.* 26, 471–501.
- Gerlich, D., Beaudouin, J., Kalbfuss, B., Daigle, N., Eils, R., and Ellenberg, J. (2003). Global chromosome positions are transmitted through mitosis in mammalian cells. *Cell* 112, 751–764.
- Gossen, M., and Bujard, H. (1992). Tight control of gene expression in mammalian cells by tetracycline-responsive promoters. *Proc. Natl. Acad. Sci. USA* 89, 5547–5551.
- Guelen, L., Pagie, L., Brassat, E., Meuleman, W., Faza, M.B., Talhout, W., Eussen, B.H., de Klein, A., Wessels, L., de Laat, W., and van Steensel, B. (2008). Domain organization of human chromosomes revealed by mapping of nuclear lamina interactions. *Nature* 453, 948–951.
- Hathaway, N.A., Bell, O., Hodges, C., Miller, E.L., Neel, D.S., and Crabtree, G.R. (2012). Dynamics and memory of heterochromatin in living cells. *Cell* 149, 1447–1460.
- Hermann, A., and Jeltsch, A. (2003). Methylation sensitivity of restriction enzymes interacting with GATC sites. *Biotechniques* 34, 924–926, 928, 930.
- Kind, J., and van Steensel, B. (2010). Genome-nuclear lamina interactions and gene regulation. *Curr. Opin. Cell Biol.* 22, 320–325.
- Kubicek, S., O'Sullivan, R.J., August, E.M., Hickey, E.R., Zhang, Q., Teodoro, M.L., Rea, S., Mechtler, K., Kowalski, J.A., Homon, C.A., et al. (2007). Reversal of H3K9me2 by a small-molecule inhibitor for the G9a histone methyltransferase. *Mol. Cell* 25, 473–481.
- Lionnet, T., and Singer, R.H. (2012). Transcription goes digital. *EMBO Rep.* 13, 313–321.
- Meuleman, W., Peric-Hupkes, D., Kind, J., Beaudry, J.B., Pagie, L., Kellis, M., Reinders, M., Wessels, L., and van Steensel, B. (2013). Constitutive nuclear lamina-genome interactions are highly conserved and associated with A/T-rich sequence. *Genome Res.* 23, 270–280.
- Moir, R.D., Yoon, M., Khuon, S., and Goldman, R.D. (2000). Nuclear lamins A and B1: different pathways of assembly during nuclear envelope formation in living cells. *J. Cell Biol.* 151, 1155–1168.
- Montes de Oca, R., Andreassen, P.R., and Wilson, K.L. (2011). Barrier-to-Autointegration Factor influences specific histone modifications. *Nucleus* 2, 580–590.
- Németh, A., Conesa, A., Santoyo-Lopez, J., Medina, I., Montaner, D., Péterfia, B., Solovei, I., Cremer, T., Dopazo, J., and Längst, G. (2010). Initial genomics of the human nucleolus. *PLoS Genet.* 6, e1000889.
- Peric-Hupkes, D., Meuleman, W., Pagie, L., Bruggeman, S.W., Solovei, I., Brugman, W., Gräf, S., Flicek, P., Kerkhoven, R.M., van Lohuizen, M., et al. (2010). Molecular maps of the reorganization of genome-nuclear lamina interactions during differentiation. *Mol. Cell* 38, 603–613.
- Peters, A.H., O'Carroll, D., Scherthan, H., Mechtler, K., Sauer, S., Schöfer, C., Weipoltshammer, K., Pagani, M., Lachner, M., Kohlmaier, A., et al. (2001). Loss of the Suv39h histone methyltransferases impairs mammalian heterochromatin and genome stability. *Cell* 107, 323–337.
- Pickersgill, H., Kalverda, B., de Wit, E., Talhout, W., Fornerod, M., and van Steensel, B. (2006). Characterization of the *Drosophila melanogaster* genome at the nuclear lamina. *Nat. Genet.* 38, 1005–1014.
- Prokocimer, M., Davidovich, M., Nissim-Rafinia, M., Wiesel-Motiuk, N., Bar, D.Z., Barkan, R., Meshorer, E., and Gruenbaum, Y. (2009). Nuclear lamins: key regulators of nuclear structure and activities. *J. Cell. Mol. Med.* 13, 1059–1085.
- Quinn, A.M., Allali-Hassani, A., Vedadi, M., and Simeonov, A. (2010). A chemiluminescence-based method for identification of histone lysine methyltransferase inhibitors. *Mol. Biosyst.* 6, 782–788.
- Raj, A., and van Oudenaarden, A. (2009). Single-molecule approaches to stochastic gene expression. *Annu. Rev. Biophys.* 38, 255–270.
- Reddy, K.L., Zullo, J.M., Bertolino, E., and Singh, H. (2008). Transcriptional repression mediated by repositioning of genes to the nuclear lamina. *Nature* 452, 243–247.
- Shevelyov, Y.Y., and Nurminky, D.I. (2012). The nuclear lamina as a gene-silencing hub. *Curr. Issues Mol. Biol.* 14, 27–38.
- Shinkai, Y., and Tachibana, M. (2011). H3K9 methyltransferase G9a and the related molecule GLP. *Genes Dev.* 25, 781–788.
- Siwek, W., Czapinska, H., Bochtler, M., Bujnicki, J.M., and Skowronek, K. (2012). Crystal structure and mechanism of action of the N6-methyladenine-dependent type IIM restriction endonuclease R.DpnI. *Nucleic Acids Res.* 40, 7563–7572.
- Strickfaden, H., Zunhammer, A., van Koningsbruggen, S., Köhler, D., and Cremer, T. (2010). 4D chromatin dynamics in cycling cells: Theodor Boveri's hypotheses revisited. *Nucleus* 1, 284–297.
- Tachibana, M., Ueda, J., Fukuda, M., Takeda, N., Ohta, T., Iwanari, H., Sakihama, T., Kodama, T., Hamakubo, T., and Shinkai, Y. (2005). Histone methyltransferases G9a and GLP form heteromeric complexes and are both crucial for methylation of euchromatin at H3-K9. *Genes Dev.* 19, 815–826.
- Thomson, I., Gilchrist, S., Bickmore, W.A., and Chubb, J.R. (2004). The radial positioning of chromatin is not inherited through mitosis but is established de novo in early G1. *Curr. Biol.* 14, 166–172.
- Towbin, B.D., González-Aguilera, C., Sack, R., Gaidatzis, D., Kalck, V., Meister, P., Askjaer, P., and Gasser, S.M. (2012). Step-wise methylation of histone H3K9 positions heterochromatin at the nuclear periphery. *Cell* 150, 934–947.
- Tumbar, T., and Belmont, A.S. (2001). Interphase movements of a DNA chromosome region modulated by VP16 transcriptional activator. *Nat. Cell Biol.* 3, 134–139.
- Tumbar, T., Sudlow, G., and Belmont, A.S. (1999). Large-scale chromatin unfolding and remodeling induced by VP16 acidic activation domain. *J. Cell Biol.* 145, 1341–1354.

- van Koningsbruggen, S., Gierlinski, M., Schofield, P., Martin, D., Barton, G.J., Ariyurek, Y., den Dunnen, J.T., and Lamond, A.I. (2010). High-resolution whole-genome sequencing reveals that specific chromatin domains from most human chromosomes associate with nucleoli. *Mol. Biol. Cell* *21*, 3735–3748.
- van Steensel, B., and de Lange, T. (1997). Control of telomere length by the human telomeric protein TRF1. *Nature* *385*, 740–743.
- van Steensel, B., and Dekker, J. (2010). Genomics tools for unraveling chromosome architecture. *Nat. Biotechnol.* *28*, 1089–1095.
- van Steensel, B., and Henikoff, S. (2000). Identification of in vivo DNA targets of chromatin proteins using tethered dam methyltransferase. *Nat. Biotechnol.* *18*, 424–428.
- Vazquez, J., Belmont, A.S., and Sedat, J.W. (2001). Multiple regimes of constrained chromosome motion are regulated in the interphase *Drosophila* nucleus. *Curr. Biol.* *11*, 1227–1239.
- Walter, J., Schermelleh, L., Cremer, M., Tashiro, S., and Cremer, T. (2003). Chromosome order in HeLa cells changes during mitosis and early G1, but is stably maintained during subsequent interphase stages. *J. Cell Biol.* *160*, 685–697.
- Wen, B., Wu, H., Shinkai, Y., Irizarry, R.A., and Feinberg, A.P. (2009). Large histone H3 lysine 9 dimethylated chromatin blocks distinguish differentiated from embryonic stem cells. *Nat. Genet.* *41*, 246–250.
- Wu, R., Terry, A.V., Singh, P.B., and Gilbert, D.M. (2005). Differential subnuclear localization and replication timing of histone H3 lysine 9 methylation states. *Mol. Biol. Cell* *16*, 2872–2881.
- Yokochi, T., Poduch, K., Ryba, T., Lu, J., Hiratani, I., Tachibana, M., Shinkai, Y., and Gilbert, D.M. (2009). G9a selectively represses a class of late-replicating genes at the nuclear periphery. *Proc. Natl. Acad. Sci. USA* *106*, 19363–19368.
- Zullo, J.M., Demarco, I.A., Piqué-Regi, R., Gaffney, D.J., Epstein, C.B., Spooner, C.J., Luperchio, T.R., Bernstein, B.E., Pritchard, J.K., Reddy, K.L., and Singh, H. (2012). DNA sequence-dependent compartmentalization and silencing of chromatin at the nuclear lamina. *Cell* *149*, 1474–1487.